2018 International Conference on Multidisciplinary Research
Track 1: STEM (Science, Technology, Engineering & Mathematics)
https://doi.org/10.26803/MyRes.2018.07

Reliability of a Directly Cooled PV/T System

Busiso Mtunzi
National University of Science and Technology,
Bulawayo, Zimbabwe

Edson Meyer
Fort Hare Institute of Technology
University of Fort Hare,
Alice, South Africa

Abstract
The objective of this paper was to quantify and evaluate the effect of water absorption on a directly cooled PV module (PV/T). A design experiment was assembled and used in analysing the performance of the directly water cooled PV module when compared to a naturally cooled PV module. The results revealed that not only the power output of the PV/T dropped, but also the series and shunt resistances of the PV/T changed, and these were found to bring about changes in the generated power. A drop in output power impacted negatively on the performance of the PV/T system. This was found to have an effect on the reliability of the PV systems, hence compounding on the system's ability to deliver the rated power during its life time. The Photovoltaic Module data considered in this paper was for a period of one year.

Keywords: Photovoltaic Thermal Module, Shunt Resistance, Reliability, Series Resistance, Performance ratio.

Introduction

In this paper, the power decline over time, also known as degradation rates for two identical PV modules were analysed. Two modules were analysed, a naturally air cooled module (M1), and a photovoltaic thermal hybrid system (PV/T), (M2). The PV/T (M2) module was cooled by water in direct contact with the back of the module.

Generally, a higher degradation rate on photovoltaic modules implies less power production. Understanding photovoltaic module degradation dynamics is important as it helps in determining the PV module's half-life; hence its reliability. Carrying out

reliability tests on new PV system designs is important as this gives PV modules' behaviour when placed outdoors.

PV modules' manufacturers and users always need to know the product's long term reliability and its performance. The investors always want to know if the project is bankable. A warranty of 20 to 25 years is usually given by most PV module manufacturers and of late, warranties of up to 30 years have been given by some manufacturers (Vazquez & Rey-Stolle, 2008). However, according to Canadian Solar (2017), by the end of year 25, the actual power output has been found to be no less than 80.7% of the labeled power output. This could mean that by the end of 30 years, the PV module power output would still be way above 50% of labelled power output. These warranties are meant for ordinary PV modules. The advent of PV hybrid systems has brought about modifications on the PV modules and the redesigned PV modules (PV/T) may/ may not meet the indicated life span. Introduction of water as a cooling media may impact negatively or positively on the PV modules, hence causing a change on the module's reliability.

In reliability engineering, it is well-known that any equipment or device would typical go through three phases during its field time (Zielnik, 2015) and these are;
Infant mortality, Random failure and Wear out failure.
The three phases are shown in figure 1:

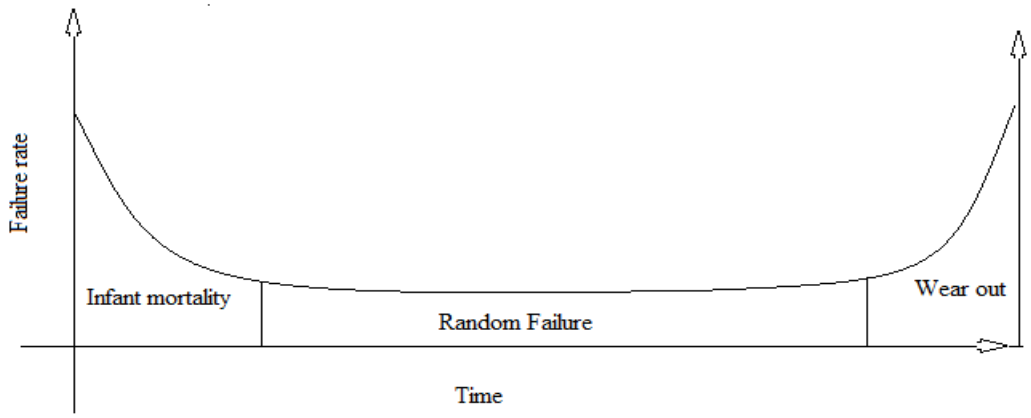

Figure 1- Classic bath tub curve showing how component failure rate can vary with time. (Zielnik, 2015)

Infant mortality region refers to early life failures of the PV modules, while random failures refer to failures that may be caused by effects such as lighting. The lightning has the same probability of occurring in the system's life, hence a constant level on the graph. The wear out failure in this case could be due to contact oxidation on the module's cells. These three phases could be applied to PV modules and are needed to help the investors and manufacturing companies to understand the module's behaviour. This information is needed to help find the gateway of improving the PV product life or its availability when in the field.

When the radiation falls onto a PV module, part of the absorbed radiation is used by the PV cells to generate electricity while the other part generates heat on the module.

The photon energy needs to be at least equal or more than the band-gap energy ΔE_g of the semiconductor (1.1eV for the crystalline silicon). Photons with energy slightly above ΔE_g are partly absorbed by the PV cells and they will generate an electron hole pair per photon. The excess energy will be transferred in the form of heat to the module. It is not all the wavelengths that generate electricity. Some of the wavelengths with energy less than ΔE_g will just pass through the PV cells and get absorbed by water, contributing towards the thermal energy. The solar cells have a high absorption coefficient and produce infrared rays. The infrared rays produced by the solar cells get reflected back by the glass causing greenhouse effect in the module hence, heating the module. The flow of heat to the back of the module passes through several thermal resistances causing a heating effect at the back of the module.
In this paper the investigations were carried out for a year.

Design

This study was designed to examine the performance of two photovoltaic modules, one naturally cooled and the other directly water cooled. A performance ratio analysis was used to check on the effects of directly water cooling of a photovoltaic module. The two modules were placed side by side facing north at an angle of Latitude tilt of 33˚S.

Two PV systems were analysed using their performance ratios and their power output. Both, the performance ratio and power output of the two modules were determined from the field measurements. The field measurements included the I-V characteristics, irradiance in the plane of array, back of module temperatures, inlet and outlet temperatures on module M2 as well as visual inspection. The block diagram showing the experimental set used in the experiment was as shown in figure 2 (Mtunzi, Meyer, Simon & Malape, 2012).

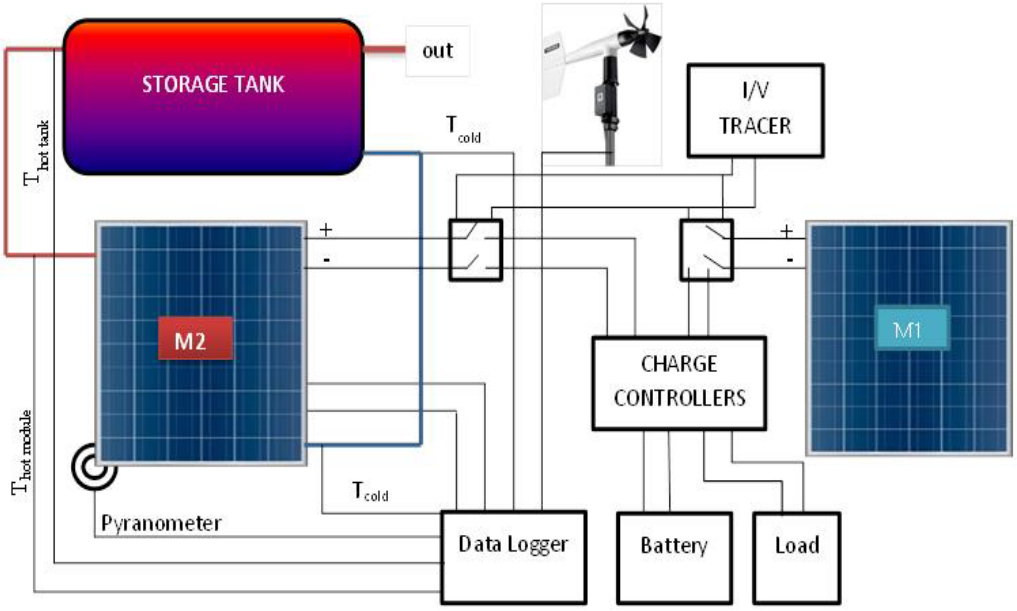

Figure 2- Schematic diagram of the PVT system with data acquisition system (Mtunzi, et al., 2012).

The respective components were put together to build up the system.

Materials and Procedure

Two photovoltaic modules used in the study were SW80 Poly/RIA type. They are polycrystalline-si technologies with 36 cells connected in series. Their name plate ratings at standard test conditions (STC) (1000 W/m^2, 25°C cell temperature and AM1.5 global spectrum) are as cited in Table 1 (SW80, 2009).

Table 1-The SW80 Poly/Ria corresponding STC and NOCT values

Performance under standard test conditions (STC)	STC **Rated**	**Performance at 800 W/m^2, NOCT Rated, AM 1.5 at 45°C**
STC Power Rating P_{mp} (W)	80.00	57.30
Open circuit voltage V_{oc} (V)	21.50	19.40
Short Circuit currency I_{sc} (A)	4.82	3.98
Peak Current I_{max} (A)	4.48	3.57
Peak Voltage V_{max} (V)	17.90	16.10
Efficiency η %	11.13	9.97
Aperture Area (m^2)	1.06x0.68	

A data-taker data logger (DT80) was used to log temperatures at the back of the modules, flow rate of water, wind speed and irradiance. Figure 4 shows the data logger used in the research.

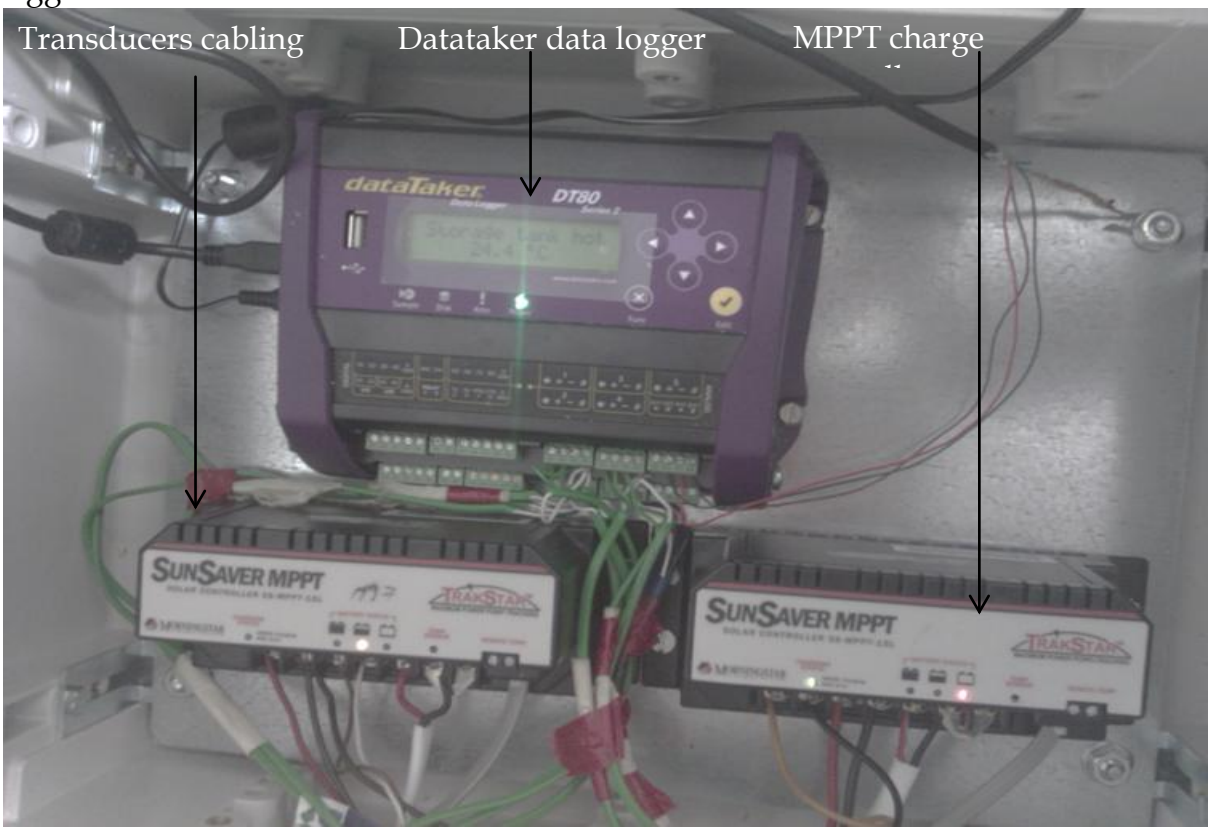

Figure 4 - Datataker datalogger DT80 and Maximum Power Point Tracking (MPPT) charge controllers.

In the study, type K thermocouples were used for temperature measurements at the back of the modules and at the inlet and outlet of the box container as well as the inlet point to the storage tank.

The solar irradiance was measured in the plane of the module using a SOZ-03 reference cell (ISO9060), Figure 5 illustrates the crystalline reference cell (SOZ-03 , 2011).

Figure 5- SOZ-03 Pyranometer

The SOZ-03 pyranometer consists of a mono-crystalline silicon cell (50 x 50 mm ²) with special solar glass. The pyranometer is laminated, hence high UV-resistance and long-term stability. The SOZ-03 also consists of an optional integrated signal amplifier (output 0-10 V) and / or temperature sensor (Pt100 or Pt1000). It was used together with a PVPM system. The accuracy of the SOZ-03 is ±5%.

The PVPM is an instrument that was used for peak power measurements and current/voltage curve tracer measurements for the PV modules. The field tests through the use of a PVPM enabled the measurements of the I-V-curves of photovoltaic modules. The device could measure and calculate the peak power Ppk, the Rs and Rp resistances directly at the place of assembly of the PV system. After a measurement the data could be stored automatically in a non-volatile storage in the instrument, PVPM, 2010. The I/V measurements were taken at 10 minutes intervals each day. With I/V characteristics then the efficiency and power output of the module were determined. Figure 6 shows the picture of a PVPM 1000C40 instrument.

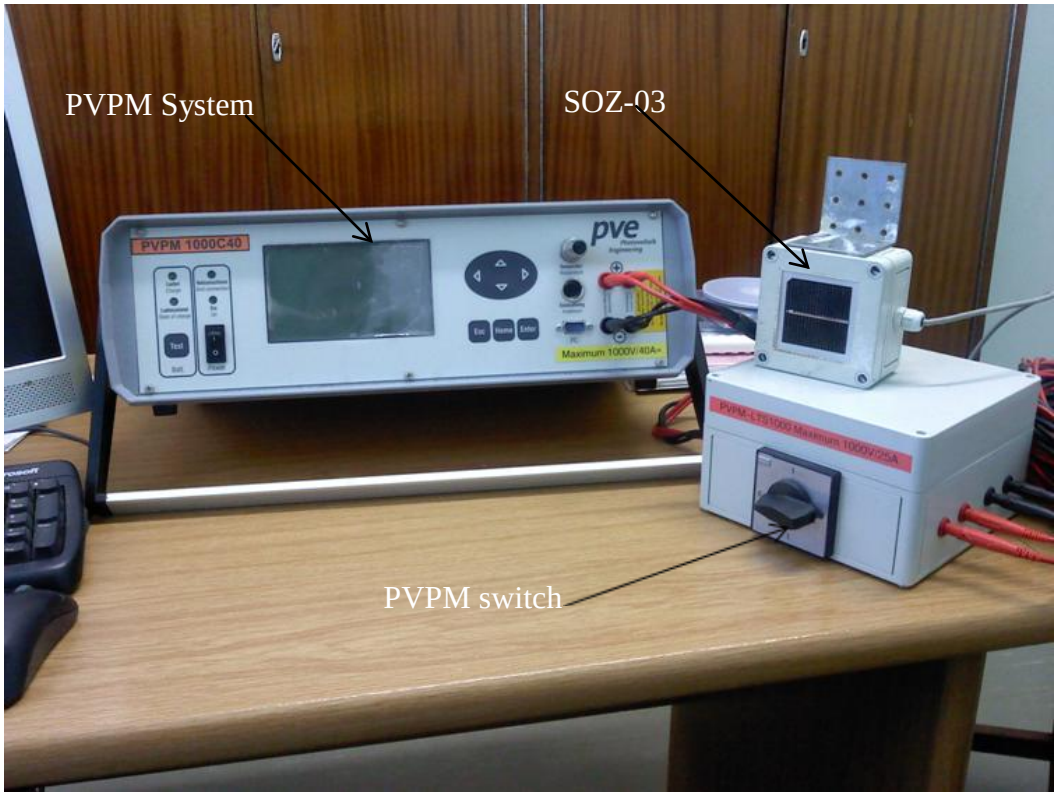

Figure 6 - The PVPM 1000C40 Instrument

The SOZ-03 measured irradiance and the PVPM used these values in converting the daily measured performance values to STC values. The peak power measurements of the PVPM have an accuracy of +/- 5% (PVPM, 2010).

All instruments were connected as illustrated in the block diagram in figure 2 and measurements were then taken.

Results and discussion

I-V Characteristics for Modules M1 and M2 (PV/T)

The PV/T showed a broader distribution of degradation rates than module M1. This was attributed to the presence of water at the back of module M2 (the PV/T). Module M2 was found to be characterised by an initial higher maximum power as compared to moduleM1. For initial measurements taken at solar noon Module M1 was found to have an initial power output of 66.19W while M2 had an initially maximum power output of 69.96W

The current voltage (I-V) measurements taken at the same time were as shown in figure 7.

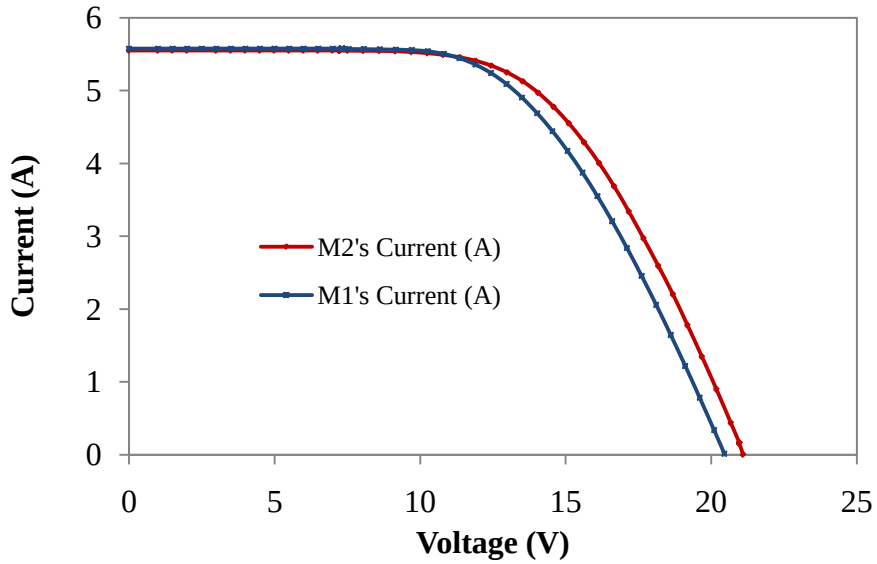

Figure 7- Initial I-V characteristics for modules M2 and M1

As shown on figure 7, the short circuit current generated by the two modules had a small difference, with M1 having a short circuit current of 5.58A and M2 giving 5.55A. A percentage difference of 0.54% between the two modules' current was noted. However the open circuit voltage of M2 was found to be 21.10V while that of M1was 20.45V. The open circuit voltage for M2 was found to be higher by 3.1%. Module M2 was also found to have a fill factor of 60% while M1 had a fill factor of 58% showing a better performance of M2 when compared to M1.

The two modules were continuously monitored every day and on the 7thmonth from the installation day, the I-V characteristics of the modules were as illustrated in figure 8.

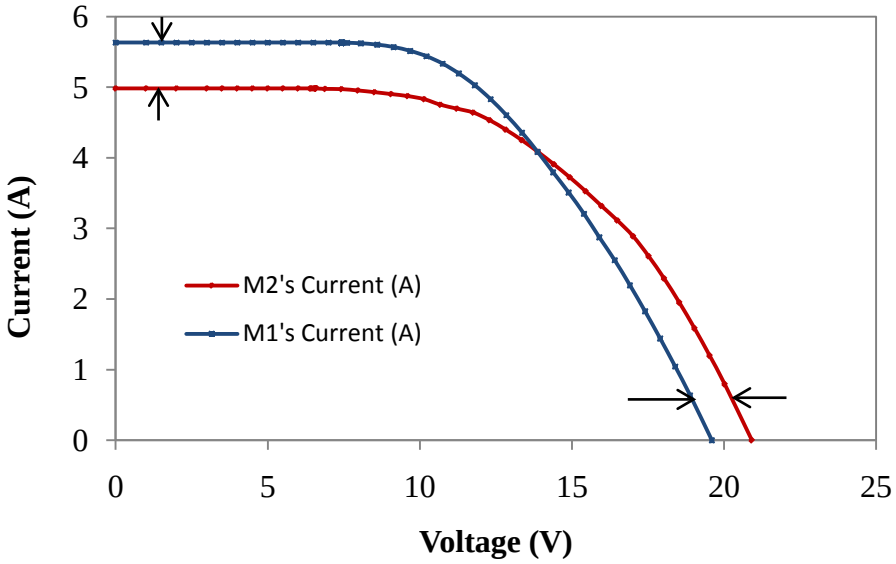

Figure 8- I-V characteristics for modules M2 and M1 taken at 12h10

The measurements were also taken around the solar noon and the irradiance was found to be 1012W/m^2. As shown in figure 8, module M2 had a lower short circuit

current (I_{sc}) of 4.98A as compared to M1's current of 5.63A. The fall in current on module M2 was due to degradation of the module. The module's degradation was likely brought about by its water absorption. A percentage drop of 11.55% in short circuit current by M2 was noted when the two modules were compared. The open circuit voltage of M2 was however found to maintain a higher value as compared to that of M1. Module M2 had an open circuit voltage of 20.9V while that of M1 was 19.6V. M1's open circuit voltage was lower than that of M2 by 6.22% and this difference was attributed to water cooling effect on module M2's back of module when compared to M1. This difference in open circuit voltage was found to have a contributing factor on the modules' fill factors. Module M1's fill factor was found to be 53.94% while that of M2 was 54.46%. Lower Fill factors were noted when these values were compared to the initial measurements. These changes were attributed to changes in the series and shunt resistances of the two modules.

As time went on, the performance of module M2 kept on dropping when compared to that of module M1. This continued performance drop contributed negatively towards the reliability of the M2 module. Figure 5 shows the changes that took place on the series and shunt resistances of the two modules. The changes in some of the module M2's electrical characteristics affected its series and shunt resistances, hence the drop in its electrical energy production. The changes in series and shunt resistances of the modules were as illustrated in Figure 9.

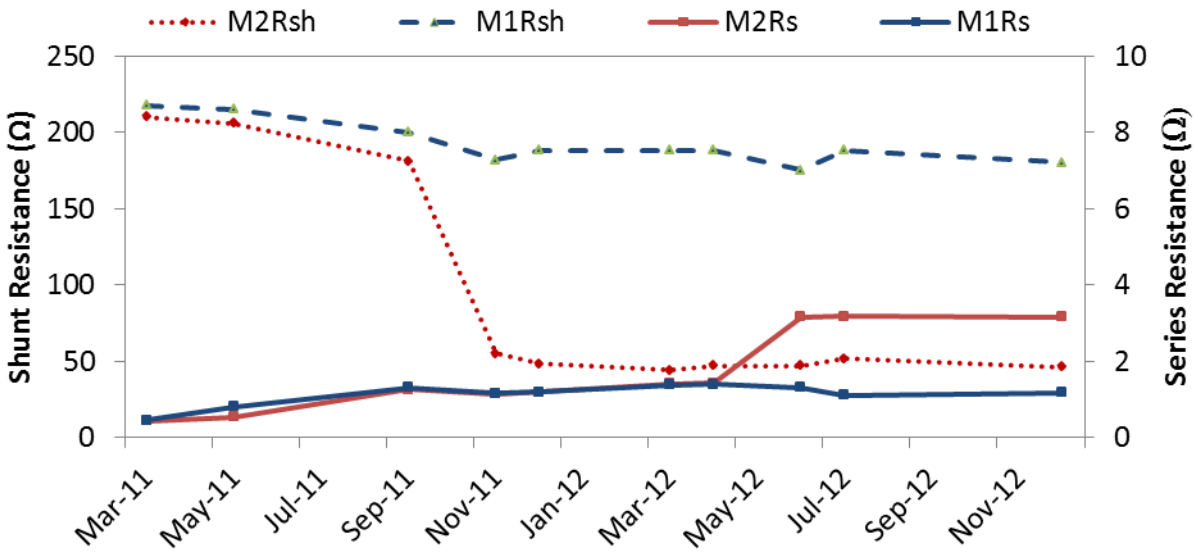

Figure 9- Series and shunt resistance variations of modules (M1) and (M2).

Figure 9 shows a 78% drop in shunt resistance for M2 as compared to 17% drop in shunt resistance of module M1. The sudden drop in power output by module M2 is therefore explained by these changes. A major drop in shunt resistance was noted towards the year end. The series resistance increased on both modules and this was assumed to be due to oxidation of the cells, hence the increase in series resistance. This sudden increased in series resistance was suspected to be due to more water absorption by the module as evidenced by the browning of cells shown in figure 10.

Figure 10- Showing oxidised cells on M2.

Not all cells were oxidised, but just a few on M2 as shown in figure 10. The oxidised cells contributed towards performance reduction in the module M2. The percentage increase in series resistance of the two modules when compared to measurements made in March 2011, were found to be 62% for M1 and 86% for M2. This shows the effect of water ingress on modules, hence a need to come up with a water tight system to avoid water ingress.

The I/V curve for module M1 in figure 11 was measured using the PVPM system (Kunz & Wagner, 2004).

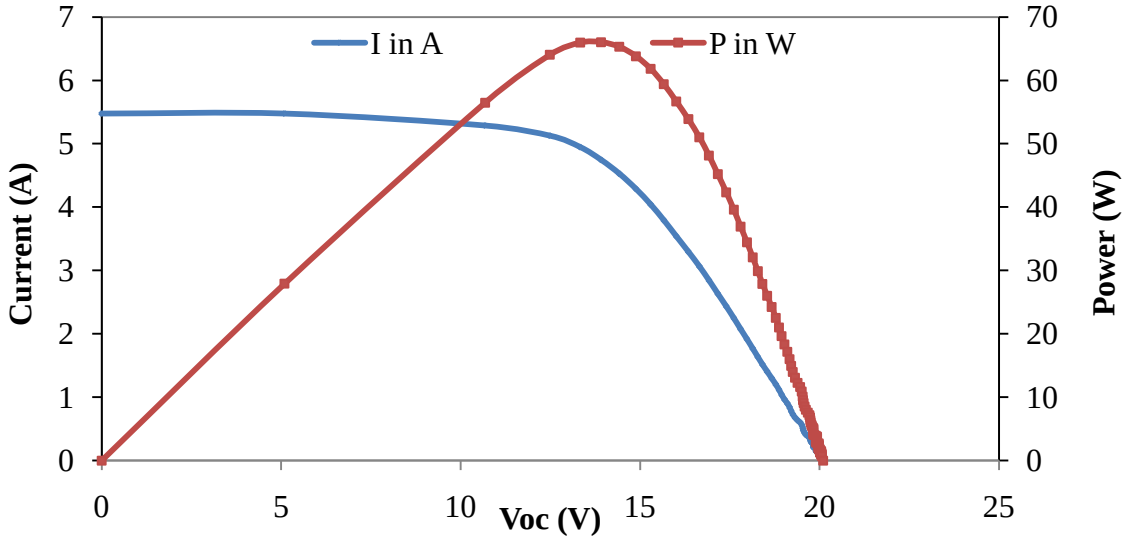

Figure 11- Year-end M1's I/V characteristic taken at 12:30pm

Figure 11 illustrates the measurements carried out towards year end. The corresponding series and shunt resistances of module M1 were found to be 1.18 Ω and 180 Ω respectively and a maximum short circuit current of 5.48A was noted. At the same time measurements were taken across module M2, and a short circuit current of 5.26A was noted as shown in figure 12.

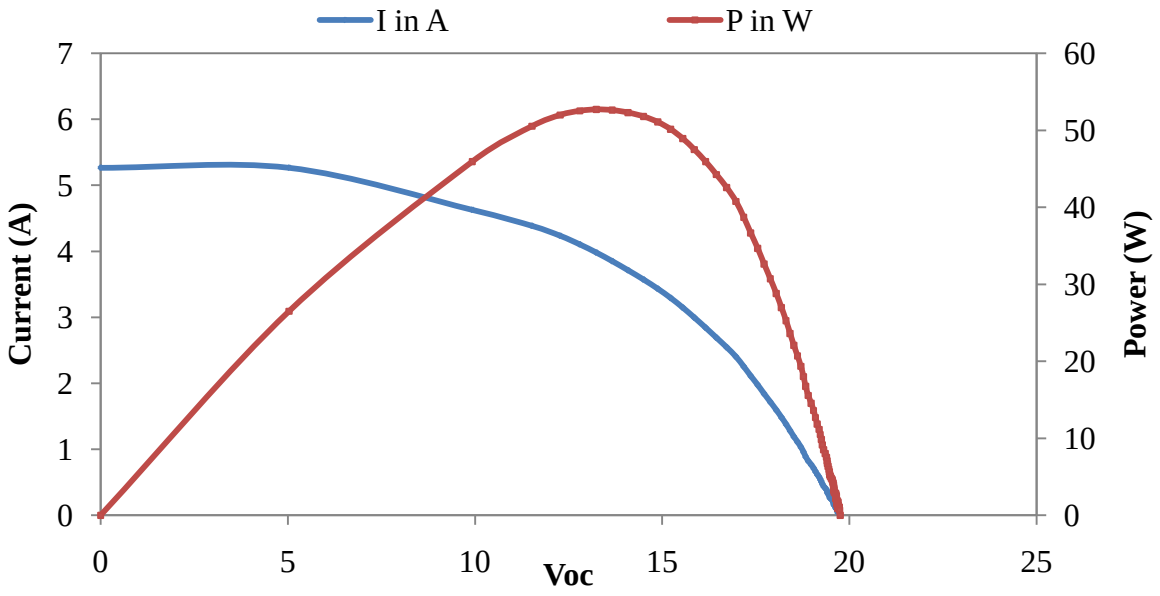

Figure 12- Year end's M2 I/V characteristic.

The series and shunt resistances of M2 were found to be 3.15 Ω and 45.97Ω respectively. This confirmed the effects of water ingress on the module M2. The series resistance of M2 increased overall by 179% while its shunt resistance decreased further by 16.42%.

To quantify power losses in the modules, the power degradation rates of the two PV systems were analysed using the performance ratios. The graphs shown in figure 13, shows the normalised graphs of the performance ratios of the two modules.

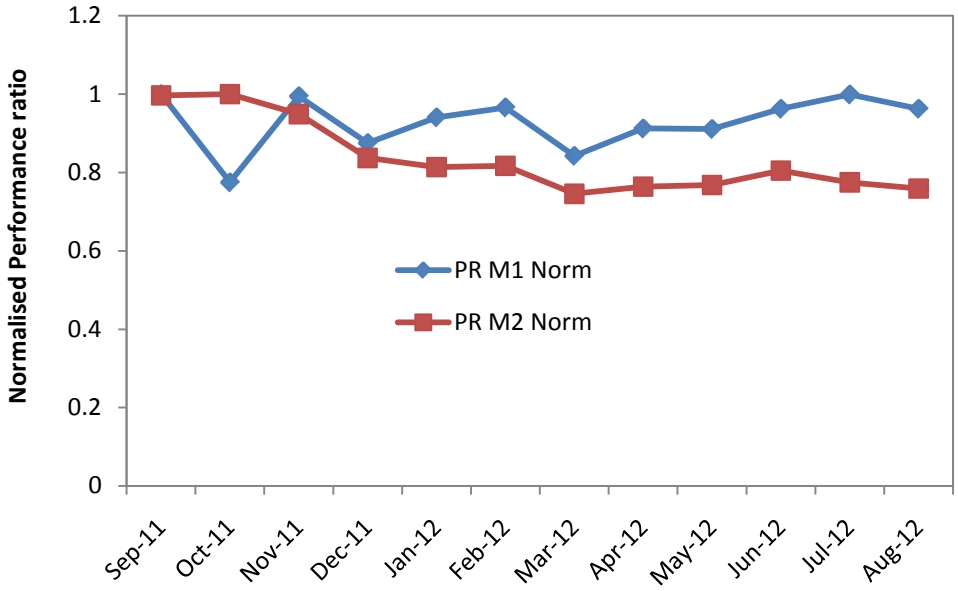

Figure 13- Normalised performance ratio of the two modules.

From figure 13, it can be seen that the performance ratio of the directly water cooled PV module M2 decreased from 100% to 76% while that of naturally cooled module decreased to 96% in a space of a year. The performance response shown in figure 13

is in agreement with findings made by Kurtz (Kurtz, 2009). With these findings, it can be concluded that, though both electrical and thermal energy could be obtained from a directly water cooled module, methods of preventing water ingress in the directly water cooled module are needed.

Conclusion

The reliability of the directly cooled module was found to be compromised by water ingress. The electrical performance ratio of the directly cooled PV module dropped by 24%, while that of a naturally cooled PV module dropped by 4%. Water ingress on the directly water cooled module contributed towards increased series resistance and decreased shunt resistance. The overall series resistance of the directly water cooled PV module increased from 0.43 Ω to 3.15 Ω, while its shunt resistance decreased from 210 Ω to 45.97Ω. To improve on the directly water cooled module's reliability, ways of preventing water ingress need to be accommodated or investigated.

References

Canadian Solar. (2017). *Limited warranty statement Photovoltaic Module products.* Retrieved from https://www.canadiansolar.com/downloads/warranties/v3.2/PV_Module_Warranty_en-v3.2.pdf

Mtunzi, B., Meyer, E.L. Simon, M. & Malape, M.A. (2012). *Variations in the I/V characteristics of directly water cooled and naturally cooled PV modules*.27th European Photovoltaic Solar Energy Conference and Exhibition. (pp 3992 – 3996). Frankfurt, Germany.

Kunz, G. & Wagner, A. (2004, June 7-11). *Internal series resistance determinated of only one I-V curve under illumination.* The 19th European Photovoltaic Solar energy conference, Paris. France. Retrieved from https://www.interempresas.net/FeriaVirtual/Catalogos_y_documentos/80319/Determinacion-de-la-Rs.pdf.

Kurtz,S. (2009). *Reliabilty issues for photovoltaic modules*. NREL/PR-520-46481. Retrieved From https://www.nrel.gov/docs/fy10osti/46481.pdf

PVPM. (2010). *Operational user's manual*. Retrieved from http://website2010.pvengineering.org/fileadmin/user_upload/download/Operation_Manual/Manual_PVPM.pdf.

SOZ-03. (nd). *Technical data*. Retrieved from: http://www.nes-datalogger.de/produkte_soz03.htm

SW80, (2014). *Sunmodule-SW-80-90-poly-RIA*. Retrieved from: http://www.rectifier.co.za/wp-content/uploads/2014/05/Sunmodule-SW-80-90-poly-RIA-en.pdf

Vazquez, M. & Rey-Stolle, P. (2008). *Photovoltaic module reliability model based on field degradation studies*. *Progress in photovoltaics: research and applications,* Wiley

interscience. Retrieved from https://onlinelibrary.wiley.com/doi/abs/10.1002/pip.

Zielnik, A.K. (2015). *White paper on Photovoltaic module weather durability and reliability testing*. Solar energy competence center. Retrieved from https://www.atlas-mts.com/-/media/ametekatlas/files/applications/photovoltaics/atlas_wp104_atlas_25plus_rev2_2015-05-12.pdf?la=en